Proceedings of the American Control Conference
San Diego, California • June 1999

FEEDBACK DESIGN FOR ROBUST TRACKING AND ROBUST STIFFNESS IN FLIGHT CONTROL ACTUATORS USING A MODIFIED QFT TECHNIQUE

David F. Thompson, John S. Pruyn, and Amit Shukla
Department of Mechanical, Industrial, and Nuclear Engineering
University of Cincinnati
P.O. Box 210072, Cincinnati, OH 45221-0072 USA

Phone: (513) 556-3693; Fax: (513) 556-3390
E-mail: david.thompson@uc.edu

ABSTRACT

The problem of dynamic stiffness of hydraulic servomechanisms has often been recognized as a significant performance issue in a variety of applications, the most notable of which includes flight control actuation. A hydraulic servomechanism is said to be "stiff" if it exhibits acceptable rejection of force disturbances within the control bandwidth. In this paper, an approach to feedback design for robust tracking and robust disturbance rejection is developed via the Quantiative Feedback Theory (QFT) technique. As a result, it is shown that reasonable tracking and disturbance rejection specifications can be met by means of a fixed (i.e., non-adaptive), single loop controller. Robust tracking and robust disturbance rejection specifications are mapped into equivalent bounds on the (parametrically uncertain) sensitivity function; hence, the frequency ranges in which tracking or disturbance rejection specifications dominate become immediately obvious. In this paper, a realistic nonlinear differential equation model of the hydraulic servomechanism is developed, the linear parametric frequency response properties of the open loop system are analyzed, and the aforementioned QFT design procedure is carried out.

1. Introduction

Dynamic stiffness of hydraulic servomechanisms is a significant performance issue in a variety of applications, the most notable of which includes aircraft flight control actuation. With the emergence of digital fly-by-wire flight control systems, sufficient control authority is now available to impact the stiffness of the closed loop system through feedback design. Recent investigations encompassing these issues include Blaignan and Skormin (1993), Raymond and Chenoweth (1993), and Kang (1994). Related applications include control of machine tools, hydraulic robots, structural control, and automotive active suspension systems. In the flight control problem, an aerodynamic flutter load on the control surface manifests itself as a force disturbance on the system. Since the disturbance does not enter the system as in the classical sense (i.e., at the plant output), a non-standard treatment of the disturbance rejection problem is required. In this paper, an approach for robust tracking and robust stiffness is developed via the Quantiative Feedback Theory (QFT) technique. Originally developed by Horowitz and Sidi (1972, 1978), the QFT methodology is aimed at designing feedback controllers so that pointwise frequency response specifications on closed loop tracking and disturbance rejection are met in spite of large parametric plant uncertainty. In particular, the QFT technique has been used effectively in a variety of flight control applications (Houpis, 1995). The methodology employed in this paper is the sensitivity-based QFT formulation due to Nordgren, Nwokah, and Franchek (1994). As a result, robust tracking and robust disturbance rejection specifications are mapped into equivalent bounds on the (parametrically uncertain) sensitivity function; hence, the frequency ranges in which tracking or disturbance rejection specifications dominate become immediately obvious.

2. Model Description and Background

In the following section, the basic differential equations describing the dynamics of a hydraulic servomechanism, in the form to be used in this paper, are described. This is followed by a description of the parametric uncertainty to be considered, as well as an examination of the open loop system characteristics.

Illustrated in Figure 1 is the basic mechanical and hydraulic system to be considered in this analysis. This set of assumptions is comparable to those most commonly used in analysis of flight control actuation systems (e.g., Raymond and Chenoweth, 1993). The system consists of an actuator piston and ram, connected to a load mass. Here, the more complex aerodynamic loads and control surface actuation mechanisms associated with an actual flight control system will be neglected in favor of a simple mass-spring-damper load. The actuator is supplied with pressurized hydraulic fluid, metered by a double-acting, zero overlap spool valve. The spool is, in turn, acted upon by a force (e.g., via a torque motor) which is driven by a voltage (or current) input. This input to the torque motor represents the open loop system (i.e., plant) input, whereas the position of the load mass represents the plant output. A force disturbance enters the system as a force acting upon the load mass. An appropriate set of nonlinear differential equations for the system is given as follows:

$$m\ddot{x} + c\dot{x} + kx = A_p(p_2 - p_1) + f_d(t) \tag{1}$$

$$m_v\ddot{x}_v + c_v\dot{x}_v + k_v x_v = f_v \tag{2}$$

$$\dot{f}_v = -\omega_c f_v + \omega_c u(t) \tag{3}$$

$$\dot{p}_2 = \frac{\beta}{V_2}\left[q_2 - q_{leak} - A_p\dot{x}\right], \quad p_2 \geq 0 \tag{4}$$

$$\dot{p}_1 = \frac{\beta}{V_1}\left[-q_1 + q_{leak} + A_p\dot{x}\right], \quad p_1 \geq 0 \tag{5}$$

$$q_{leak} = \sqrt{(2/\rho)}\, C_d\, A_{leak} \sqrt{|p_2 - p_1|}\, sign(p_2 - p_1) \tag{6}$$

and for $x_v > 0$,

$$q_2 = \sqrt{(2/\rho)}\, C_d\, D_v\, x_v \sqrt{|p_{line} - p_2|}\, sign(p_{line} - p_2) \tag{7}$$

$$q_1 = \sqrt{(2/\rho)}\, C_d\, D_v x_v \sqrt{p_1} \tag{8}$$

and where $q_1 = q_2 = 0$ for $x_v = 0$ corresponds to the assumed zero-overlap condition. State variables for the problem include f_v, force on spool valve; p_1, pressure; p_2, pressure; v, load velocity; v_v, spool velocity; x, load position; and x_v, spool

position. Operating point parameter values for the system and additional details are indicated in Thompson et al. (1999). This set of parameters, adapted from available references (including McLean, 1990), is representative of an actuator for a small control surface in a high performance jet aircraft application. These parameters include A_{leak}, leakage area; A_p, piston area; β, bulk modulus; c, load damping constant; C_d, discharge coefficient; c_v, spool damping constant; D_v, spool diameter; k, load stiffness; k_v, spool spring stiffness; m, load mass; m_v, spool mass; p_{line}, line pressure; $(p_1)_0$, nominal cylinder pressure; $(p_2)_0$, nominal cylinder pressure; $(\Delta p)_0$, nominal pressure differential; V_1, cylinder volume; V_2, cylinder volume; $(x_v)_0$, nominal valve position; ω_c, torque motor corner frequency.

A linear robust stability and robust performance analysis is developed based upon an operating point corresponding to $p_{line}=20000$ kPa (3000 psi) line pressure. State variables used in the linear model are hereinafter perturbation values, i.e., $\Delta p_1 = p_1 - (p_1)_0$; the "$\Delta$" is subsequently omitted for conciseness. Bias terms, i.e., due to the constant line pressure p_{line} are eliminated as a result. The linearized flow relationships from (1) - (8) are given below, assuming $x_v \geq 0$.

$$q_1 = c_{1_x} x_v + c_{1_p} p_1 \tag{9}$$

$$q_2 = c_{2_x} x_v - c_{2_p} p_2 \tag{10}$$

$$q_{leak} = c_{leak}(p_2 - p_1) \tag{11}$$

where, e.g.,

$$c_{2_x} = \frac{1}{2}\sqrt{\frac{2}{\rho}}\, C_d \pi D_v (x_v)_0 \sqrt{\frac{1}{p_{line} - (p_2)_0}} \tag{12}$$

$$c_{2_x} = \sqrt{\frac{2}{\rho}}\, C_d \pi D_v \sqrt{p_{line} - (p_2)_0} \tag{13}$$

Upon substitution and rearrangement, a set of linear first-order state equations are obtained, in terms of the control input $u(t)$ (torque motor voltage), disturbance (force) input $f_d(t)$, and output x (load position):

$$\dot{f}_v = -\omega_c f_v + \omega_c u(t) \tag{14}$$

$$\dot{x} = v \tag{15}$$

$$\dot{v} = \frac{1}{m}\left[-kx - cv - A_p p_1 + A_p p_2\right] + \frac{1}{m} f_d(t) \tag{16}$$

$$\dot{x}_v = v_v \tag{17}$$

$$\dot{v}_v = \frac{1}{m}\left[f_v - k_v x_v - c_v v_v\right] \tag{18}$$

$$\dot{p}_1 = \frac{\beta}{V_1}\left[A_p v - c_{1_x} x_v - (c_{1_p} + c_{leak}) p_1 + c_{leak} p_2\right] \tag{19}$$

$$\dot{p}_2 = \frac{\beta}{V_2}\left[-A_p v + c_{2_x} x_v + c_{leak} p_1 - (c_{2_p} + c_{leak}) p_2\right] \tag{20}$$

These first-order equations can be immediately cast in the standard state-space form. A transfer function model of the open loop system may be obtained by reduction of the Laplace transforms of Equations (14) - (20), which leads to the following expression:

$$X(s) = \left[\frac{\omega_c A_p(\gamma_3 s + \gamma_4)}{D(s)(m_v s^2 + c_v s + k_v)(s + \omega_c)}\right] U(s) + \left[\frac{(s+\alpha_{11})(s+\alpha_{22}) - \alpha_{12}\alpha_{21}}{D(s)}\right] F_d(s) \tag{21}$$

hereinafter denoted as

$$X(s) = P(s)\, U(s) + P_d(s)\, F_d(s) \tag{22}$$

with plant transfer function $P(s)$ and disturbance transfer function $P_d(s)$, and where $U(s)$ denotes the Laplace transform of the time function $u(t)$, etc. Note that the transfer function magnitude $|F_d(j\omega)/X(j\omega)| = |P_d(j\omega)|^{-1}$ (i.e., force per unit displacement), represents the stiffness of the system in open loop.

The linear system (14)-(20) is modeled to include parametric uncertainty in nominal pressure differential across the actuator piston $(\Delta p)_0$, nominal spool position $(x_v)_0$, fluid bulk modulus β, and torque motor cutoff frequency ω_c. The parameters are assumed to be independently variable. Operating-point values and corresponding uncertainty ranges are given in Table 1 as follows:

Table 1: Operating point values and parameter ranges:

Parameter	Operating Pt.	Minimum	Maximum
$(\Delta p)_0$	$2.225(10^6)$	$0.5\,(\Delta p)_0$	$10.0\,(\Delta p)_0$
$(x_v)_0$	$0.1(10^{-3})$	$0.1\,(x_v)_0$	$2.0\,(x_v)_0$
β	$7.0(10^8)$	0.5β	1.5β
ω_c	$2\pi(100)$	$0.5\,\omega_c$	$2.0\,\omega_c$

The uncertain parameters are subsequently grouped into a vector, denoted as α. In the QFT design problem, a reference or "nominal" parameter vector, denoted as α_0, is required. This α_0, can be chosen as any point in the uncertainty set. Examination of pole-zero data over the uncertainty set reveals that the plant set is stable and minimum phase, although the techniques to be presented subsequently are not so limited. The Quantitative Feedback Theory (QFT) technique is now introduced as a method for designing feedback controllers to achieve explicit, pointwise closed loop frequency domain specifications in the face of parametric and non-parametric uncertainty.

3. Quantitative Feedback Theory: Background

The Quantitative Feedback Theory methodology stems from Horowitz and Sidi (1972). The methodology employed in this paper is the sensitivity-based QFT formulation given in Nordgren, Nwokah, and Franchek (1994). Further details regarding stabilizability and existence conditions for QFT controllers are given in Jayasuriya and Zhao (1994). A modified approach leading to reduced conservatism was outlined in Thompson and Pruyn (1998). Related work on traditional and sensitivity-based QFT design formulations includes Zhao and Jayasuriya (1994), Chait, Borghesani, and Zheng (1995). Considering the standard single-input, single-output (SISO) two degree-of-freedom feedback configuration with parametric plant transfer function $P(\alpha,s)$,

controller $G(s)$, prefilter $F(s)$, reference input $R(s)$ and disturbance $D(s)$, the parameter vector is denoted as $\alpha \in \Omega \subset R^{n_\alpha}$ where Ω is a set of closed intervals in R^{n_α}. The closed loop transfer function is thus $T(\alpha,s) = P(\alpha,s)G(s)/(1+P(\alpha,s)G(s))$ and the sensitivity function is correspondingly $S(\alpha,s) = 1/(1+P(\alpha,s)G(s))$.

4. Problem Definition and Performance Specifications

As noted in the model development of Section 2, the open loop system response is given, now in terms of the parametrically uncertain plant, as $X(\alpha,s) = P(\alpha,s)U(s) + P_d(\alpha,s)F_d(s)$, with control input $U(s)$ and filtered disturbance $P_d(\alpha,s)F_d(s)$. In the two degree-of-freedom feedback configuration of Figure 2, the closed loop system response becomes

$$X(\alpha,s) = \frac{F(s)P(\alpha,s)G(s)}{1+P(\alpha,s)G(s)}R(s) + \frac{P_d(\alpha,s)F_d(s)}{1+P(\alpha,s)G(s)} \tag{23}$$

with reference input $R(s)$. The closed loop compliance (reciprocal stiffness), is given by $|X(\alpha,j\omega)/F_d(j\omega)| = |P_d(\alpha,j\omega)/(1+P(\alpha,j\omega)G(j\omega))|$. A bound on minimum actuator stiffness (i.e., maximum compliance) can thus be posed as the following inequality:

$$\max_{\alpha}\left|\frac{P_d(\alpha,j\omega)}{1+P(\alpha,j\omega)G(j\omega)}\right| \le M_k(\omega) \;\forall\alpha\in\Omega, \forall\omega \tag{24}$$

where the quantity $(M_k(\omega))^{-1}$ is introduced as an *a priori* specified lower bound on actuator stiffness. A sufficient condition can then be stated as a standard robust disturbance rejection problem in the following form:

$$\max_{\alpha}\left|\frac{1}{1+P(\alpha,j\omega)G(j\omega)}\right| \le \frac{M_k(\omega)}{\max_{\alpha}|P_d(\alpha,j\omega)|} \equiv M_D(\omega) \tag{25}$$

For this problem, the bound $M_k(\omega)$ is chosen (with some trial and error examination of the resultant problem) as

$$M_k(\omega) = 3.0(10^{-7})\left|(1+\frac{j\omega}{60})^2/(1+\frac{j\omega}{600})^2\right| \tag{26}$$

A plot of $(M_k(\omega))^{-1}$ and the open loop stiffness magnitude $|P_d(\alpha,j\omega)|^{-1}$ is given in Figure 3, showing that the open loop system does not meet the stiffness requirement for $\omega < 40$ rad/s. In addition to the disturbance rejection specification, one of the key steps in the formulation of a well-posed QFT problem lies in the development of a realistic set of robust tracking specifications. In this case, a set of tracking specifications adapted from Kang (1994) is used:

$$a(j\omega) = \frac{1}{(1+\frac{j\omega}{3})(1+\frac{j\omega}{10})} \tag{27}$$

$$b(j\omega) = \frac{(1+\frac{j\omega}{50})(1+\frac{j\omega}{400})}{(1+\frac{j\omega}{45})(1+\frac{j\omega}{60})(1+\frac{j\omega}{2000})} \tag{28}$$

These specifications allow for a variation in closed loop magnitude of less that 1 db at $\omega = 1$ rad/s, with an allowable variation of 12 db at $\omega = 10$. The stiffness bound $M_D(\omega)$ on $\max|S(\alpha,j\omega)|$ is dominant in the frequency range of approximately $3 \le \omega \le 50$ rad/s, whereas the tracking-induced bound $M_T(\omega)$ dominates at lower and higher frequencies.

5. QFT Bounds and Controller Design

In this section, we develop the open loop transfer function bounds $q(\omega)$ and introduce the QFT controller synthesis or "loop shaping" problem. Based upon the sensitivity function bound $M(\omega)$, the open loop robust performance and stability bounds $q(\omega)$ are computed. In order to obtain a feasible QFT design, $L_0(j\omega)$ must be shaped (via design of the controller $G(j\omega)$) so that $|L_0(j\omega)| \ge q(\angle L_0(j\omega),\omega)$ for all frequencies at which the bound q is a single-valued function of phase angle. In the case of multiple-valued bounds, $L_0(j\omega)$ must lie exterior to the contour.

The process of synthesizing such an $L_0(j\omega)$ is the "loop shaping" process of QFT design, which can generally be carried out by means of classical Bode analysis (e.g., straight-line approximation) with systematic trial-and-error. Following the systematic Bode analysis approach, perhaps one of the most effective methods is to initially cancel some or all of the (stable) nominal plant dynamics, adding high frequency poles as necessary to make the controller proper or strictly proper. In addition, it is usually desirable to add an integrator term to make the system type one, if it is not initially so. Such a controller is found to be

$$G(s) = \frac{2.75(10^4)(1+\frac{s}{2.0})(1+\frac{s}{314})(1+\frac{250s}{175625}+\frac{s^2}{175625})}{s(1+\frac{s}{2000})(1+\frac{s}{2000})(1+\frac{2000s}{10^8}+\frac{s^2}{10^8})} \tag{29}$$

The numerator of this controller effectively cancels the nominal plant dynamics within the control bandwidth. This controller is sufficient to stabilize the nominal closed loop system; however, there is insufficient gain to meet robust performance specifications for $\omega < 100$ rad/s (i.e., $L_0(j\omega)$ violates the QFT bounds $q(\omega)$ at these frequencies), and it is evident that a higher-order controller is required. The subsequent process can be described as that of adding a series of lead or lag terms (of the form $(1+s/z)/(1+s/p)$) in a systematic fashion, so that the open loop design bounds $q(\omega)$ are met with a minimum of over-design, yet without excessive controller order. After several iterations, the following design is found acceptable:

$$G(s) = \frac{1.94(10^6)(1+\frac{s}{3.7})(1+\frac{s}{4})(1+\frac{s}{5})(1+\frac{s}{50})}{s(1+\frac{s}{0.63})(1+\frac{s}{12})(1+\frac{s}{25})(1+\frac{s}{500})} \times \frac{(1+\frac{s}{314})(1+\frac{250s}{175625}+\frac{s^2}{175625})}{(1+\frac{s}{2000})(1+\frac{16000s}{10^8}+\frac{s^2}{10^8})} \tag{30}$$

For additional details, refer to Thompson et al. (1999). Figure 4 shows the resultant sensitivity function magnitudes $|S(\alpha,j\omega)|$. Because of the small over-design of (47), the optimization-based

approach developed in Thompson and Nwokah (1994) was found to yield only a marginal reduction in high frequency gain when applied to this problem; this would suggest that any gain in economy of bandwidth could only be achieved with a further increase in order controller.

6. Closed Loop Analysis

The final step in the two degree-of-freedom design process is selection of the prefilter F. This allows the set-point response to be adjusted so that the closed loop tracking requirement $|a(j\omega)| \le |F(j\omega)\, L(\alpha, j\omega)/(1+L(\alpha, j\omega))| \le |b(j\omega)|$ is met. For (47) an acceptable prefilter is found to be

$$F(s) = (1+s)/((1+s/0.9)(1+s/20)) \qquad (31)$$

Closed loop Bode magnitude plots for all α are given in Figure 5. Although some of the apparent conservatism stems from the dominance of the stiffness specification (i.e., on $3 \le \omega \le 50$), the remaining conservatism is inherent in the sensitivity-based formulation (Nordgren, Nwokah, and Franchek, 1994). For further details, see Thompson and Pruyn (1999). The closed loop stiffness magnitude $|P_d(\alpha, j\omega)/(1+P(\alpha, j\omega)G(j\omega))|^{-1}$ and its specification are shown in Figure 6, indicating that this design goal is met.

7. Conclusion

The principal objective of this paper has been to demonstrate that the actuator stiffness problem can be posed as a classical disturbance rejection problem (by means of the filtered disturbance $P_d(\alpha, s)F_d(s)$), and that a combined robust stiffness and robust tracking problem could be formulated and solved in a straightforward manner with a fixed, single-loop controller within the standard QFT framework. As indicated in the Introduction, the focus of this study has been upon linear parametric robustness characteristics; some form of adaptation or gain scheduling would generally be required in an actual implementation to cope with large changes in the operating point. Other techniques for enhancement of stiffness, performance, and/or stability in flight control actuation systems have included feedforward control (Blaignan and Skormin, 1993) and feedback of pressure differential (Raymond and Chenoweth, 1993). Incorporation of these techniques (which would act to increase control authority) within the QFT-based approach described in this paper would no doubt lead to additional performance gains. This should be a straightforward extension of the methodology and is worthy of additional study.

REFERENCES:

Blaignan, V.B., and Skormin, V.A., 1993, "Stiffness enhancement of flight control actuator," *IEEE Trans. on Aerospace and Electronic Systems*, **29**, 380-90, 1993.

Chait, Y., Borghesani, C., and Zheng, Y., 1995, "Single-loop QFT design for robust performance in the presence of non-parametric uncertainties," *J. of Dynamic Systems, Measurement, and Control*, **117**, 420-5.

Horowitz, I.M., and Sidi, M., 1972, "Synthesis of feedback systems with large plant ignorance for prescribed time domain tolerance," *Int. J. of Control*, **16**, 287-309.

Horowitz, I.M., and Sidi, M., 1978, "Optimum synthesis of nonminimum-phase feedback systems with parameter uncertainty," *Int. J. of Control*, **27**, 361-86.

Houpis, C.H., Ed., 1995, "Quantitative feedback theory (QFT) for the engineer," WL-TR-95-3061, Flight Dynamics Directorate, Wright Laboratory, Wright-Patterson AFB, OH.

Jayasuriya, S., and Zhao, Y., 1994, "Stability of quantitative feedback designs and the existence of robust QFT controllers," *Int. J. of Robust and Nonlinear Control*, **4**, 21-46.

Kang, K. H., 1994, "Electro-hydrostatic actuator controller design using Quantitative Feedback Theory," M.S. Thesis, Department of Electrical Engineering, Air Force Institute of Technology, Wright-Patterson AFB, OH, AFIT/GE/ENG/94D-18.

McLean, D., 1990, *Automatic flight control systems*, Englewood Cliffs, NJ: Prentice Hall.

Nordgren, R.E., Nwokah, O.D.I., and Franchek, M.A., 1994, "New formulations for Quantitative Feedback Theory," *Int. J. of Robust and Nonlinear Control*, **4**, 47-64.

Raymond, E.T., and Chenoweth, C.C., 1993, *Aircraft flight control actuation system design*, Warrendale, PA: Society of Automotive Engineers.

Thompson, D.F., and Nwokah, O.D.I., 1994, "Analytic loop shaping methods in Quantitative Feedback Theory," *J. of Dynamic Systems, Measurement, and Control*, **116**, 169-77.

Thompson, D.F., and Pruyn, J.S., 1999, "On characterizing traditional and sensitivity-based formulations for Quantitative Feedback Theory," in press, *Int. J. of Control*.

Thompson, D.F., Pruyn, J.S., and Shukla, A., 1999, "Feedback design for robust tracking and robust stiffness in flight control actuators using a modified QFT technique" in review, *Int. J. of Control*.

Zhao, Y., and Jayasuriya, S., 1994, "On the generation of QFT bounds for general interval plants," *J. of Dynamic Systems, Measurement, and Control*, **116**, 618-27.

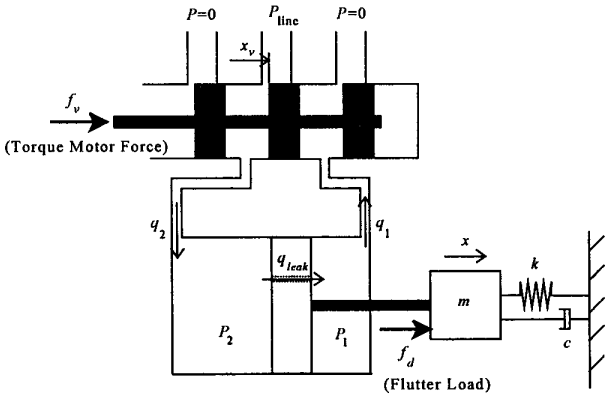

Figure 1: Schematic for the hydraulic servomechanism. The voltage input exerts a force f_v on the valve spool.

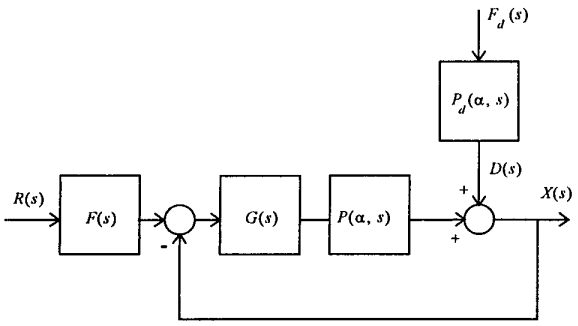

Figure 2: Illustration of the two degree-of-freedom feedback structure with disturbance filter P_d.

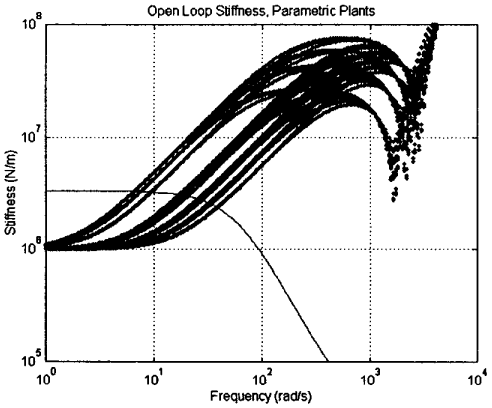

Figure 3: Magnitude plot of open loop stiffness $|P_d(j\omega)|^{-1}$ and the closed loop stiffness specification (43).

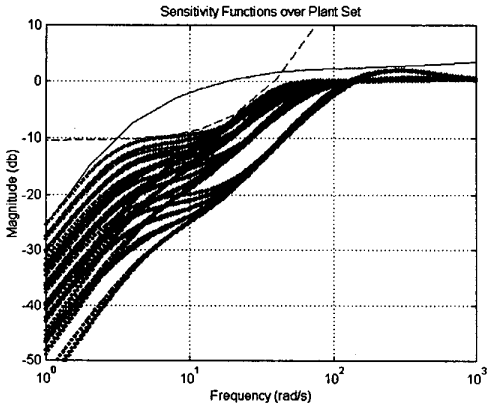

Figure 4: Plot of sensitivity functions $|S(\alpha, j\omega)|$ with the feasible controller (47). (Solid upper bound – tracking; dashed upper bound – stiffness.)

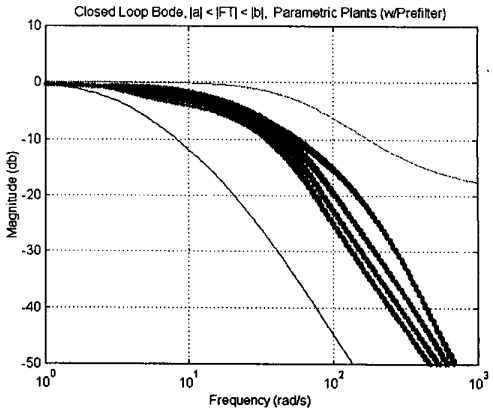

Figure 5: Closed loop frequency response magnitudes $|F(j\omega)\ T(\alpha, j\omega)|$ for the system with the tracking and stiffness-based controller (47).

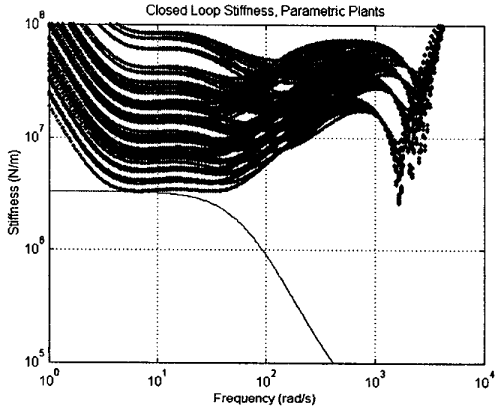

Figure 6: Closed loop stiffness magnitude $\left|P_d(\alpha, j\omega) / (1 + P(\alpha, j\omega)\ G(j\omega))\right|^{-1}$ using the controller (47).